Population index reloaded

Sirko Molau

Abenstalstr. 13b, 84072 Seysdorf, Germany
sirko@molau.de

This paper describes results from the determination of population indices from major meteor showers in 2014–2015. In many cases we find outliers that cannot be explained easily by the data set or the used algorithm. Alternative approaches are presented to check, if the outliers are real or instrumental errors. There is no conclusive result, though. An outlook is given, how the testing setup may be improved.

1 Introduction

The population index, or r-value, describes the brightness distribution of a meteor shower. More specifically, it represents the increase in total meteor count when the limiting magnitude (lm) improves by one mag. The population index is vital for the calculation of zenithal hourly rates (ZHRs) and flux densities. It can also be converted into the mass index s, which describes the particle size distribution in a meteoroid stream.

Historically, the population index was primarily obtained from visual observations. In 2014 the author presented a novel procedure to calculate the population index from video observations (Molau et al., 2014). It was not based on meteor counts in different brightness classes as in the traditional approach, but rather on meteor counts of observing intervals with different limiting magnitude.

The algorithm can be summarized as follows:

- Sort all 1-min observing intervals of all video cameras by their limiting magnitude.
- Split the data set into four lm classes such that each class has about the same effective collection area.
- Calculate flux density vs. population index graphs for each lm class (*Figure 1*)
- Select the population index that fits best to all classes.

In practice, a Poisson distribution is used to weight the contribution on each lm class (*Figure 2*).

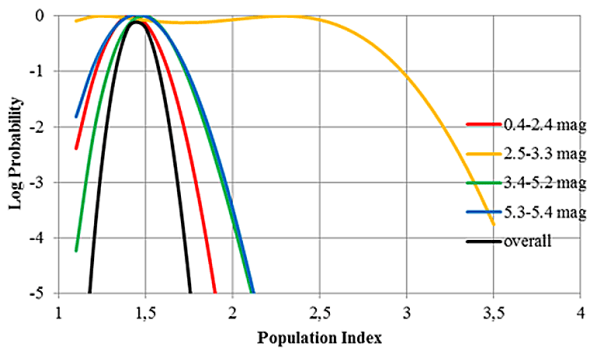

Figure 1 – The population index is determined by calculating the dependency of the flux density from the population index for different limiting magnitude classes, and select the r-value where the graphs intersect.

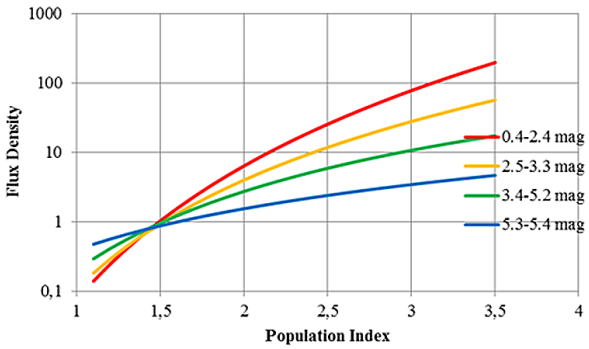

Figure 2 – A Poisson distribution is used to weight the different lm classes when selecting the best r-value.

2 Recent results

Based on the new procedure, population index profiles have been obtained for different major meteor showers and sporadic meteors in 2014 and 2015. In fall 2014, the obtained r-values for sporadic meteors were typically 2.5 or below, whereas they were above 2.5 in spring 2015. The population index for meteor showers was always smaller than for sporadic meteors, which matches our expectation since shower meteors are typically brighter.

It turned out, that individual lm class graphs intersect often better for smaller showers with fewer meteors than for major showers. The population index profiles are typically quite smooth over several days, but in many cases there are also significant outliers.

The r-value of Perseids 2014 (*Figure 3*) is below 2.0 during the full observing interval. There is a significant outlier on August 9/10 even though we have a perfect data set for that night. The calculated sporadic population index is below 2.0 on August 3, 13 and 16.

The population index profile of the Orionids in October 2014 (*Figure 4*) is almost identical to the profile of sporadic meteors up to the peak. Looking only at the Orionids one could think there is a perfect profile with a nice dip towards the maximum, but sporadic meteors show in fact the same dip which questions if this feature is real or just an instrumental error.

The Leonids (*Figure 5*) are clearly brighter than the sporadic meteors in all nights of November 2014 but the maximum night (November 18/19).

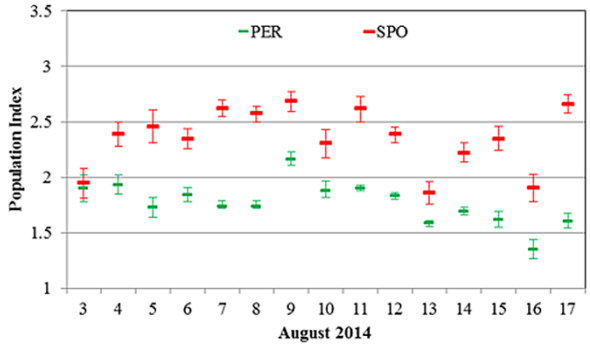

Figure 3 – Population index profile of the Perseids and the sporadic meteors in August 2014.

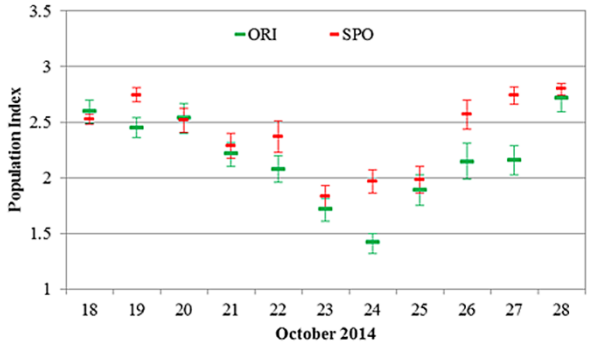

Figure 4 – Population index profile of the Orionids and the sporadic meteors in October 2014.

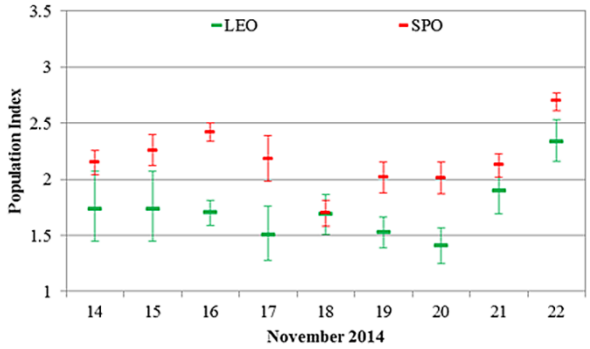

Figure 5 – Population index profile of the Leonids and the sporadic meteors in November 2014.

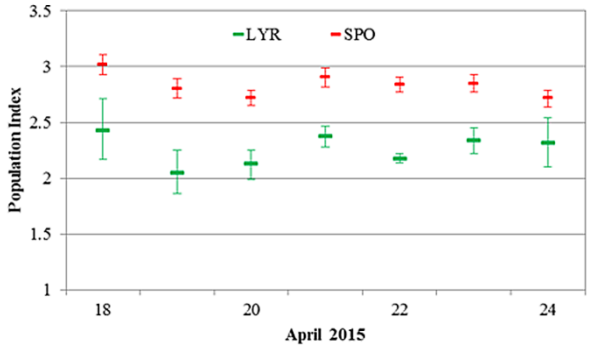

Figure 6 – Population index profile of the Lyrids and the sporadic meteors in April 2015.

Also the Lyrids of April 2015 show a significantly lower population index than the sporadic meteors during the whole activity interval (*Figure 6*). The sporadic population index has increased to almost 3.0. If both profiles are compared in detail, we can see the same tendency, e.g. both graphs are moving up and down at the same time.

3 Discussion

At first the root cause for the outliers was searched in the algorithm and data set. In order to exclude shortcomings of the algorithm (e.g. imperfect number of lm classes, inaccurate limiting magnitude calculation under poor conditions), the following tests were conducted:

- Computing the r-value with a different number of lm classes.
- Fixing the boundaries of the different lm classes over all nights.
- Introducing a lower limiting magnitude limit.

The impact of individual cameras on the result was tested by:

- Leaving-one-out analysis, i.e. iteratively excluding each camera once from the analysis.
- Using only cameras that were active all nights.

All of these tests did not significantly change the result and could not explain the observed outliers.

Also the data set itself was analyzed in detail, whether it was too small or affected by poor observing conditions, but once more this could not explain the observation.

Finally, it was checked whether there is an independent confirmation for the observed outliers. In some cases there was an obvious correlation with the sporadic population index profile, which hints on problems with the analysis procedure, but not in all cases. Comparable analyses from visual observations were unfortunately not available. So it was decided to analyze the video data set in a different way.

4 Alternative approach

In case of visual observations, the population index is obtained from meteor brightness distributions. The author has argued before, that this is a bad choice for video observations. Individual meteor brightness estimates show large errors since they are based on pixel sums in noisy video frames. Nearby stars or other bright objects impact the calculated brightness, and there is typically no correction for variations in the stellar limiting magnitude due to clouds or haze (Molau et al., 2014).

Furthermore the true population index profile is unknown, since there is no reference observation. For this reason it was decided to use the sporadic meteors from March 2015 as reference. At this time of year, there is no bias from meteor showers and the r-value should be fairly constant. The population index profile confirms this assumption (*Figure 7*), and also here we find clear outliers (downwards on March 14 and 28, upwards on March 15 and 26) which cannot be explained by the underlying data set.

In the first step, this profile was matched against the mean magnitude of the sporadic meteors (*Figure 8*). Note that this is a rogue measure just as if we would compute a visual

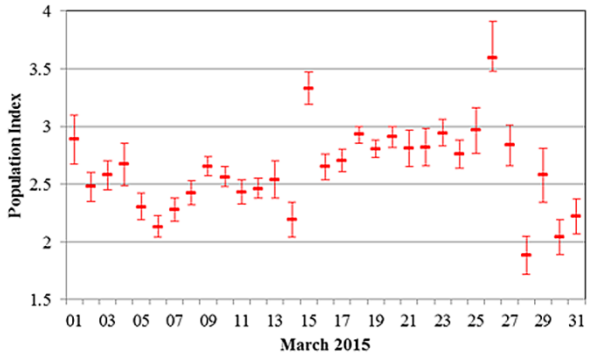

Figure 7 – Population index profile of sporadic meteors in March.

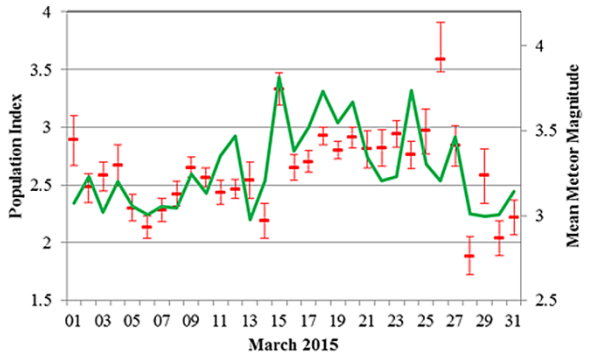

Figure 8 – Comparison of the mean meteor brightness with the population index profile.

ZHR without any lm correction. However, the advantage of that simple measure is that it does not depend on the calculation of the limiting magnitude or the effective collection areas, which could be the source of systematic errors.

The similarity of the two graphs becomes obvious at first glance. The correlation factor is about 0.7. The overall shape of both graphs is similar. Some outliers disappeared and others are confirmed. However, it should be noted that the graphs are plotted against different axes. The secondary y-axis was scaled such that the mean and variance of both graphs are identical. That is, a direct conversion from the mean meteor magnitude into the population index is not possible.

In the next step, the mean meteor brightness was replaced by the mean difference Δm between the meteor brightness and the limiting magnitude (*Figure 9*). This measure is similar to the value used for visual observations. It accounts for the limiting magnitude and seems to adapt slightly better to the population index profile, but the correlation coefficient is similar. What is still needed is a formula to convert Δm into r.

This formula depends on the detection probability of meteors. From visual double-count observations it was once concluded, that the detection probability is a function of the distance from the center of field of view (fov) and Δm in case of visual observers (Koschak and Rendtel, 1990). There is a linear dependency between the log probability *log p* and Δm (*Figure 10*). For video observations, the distance from the center of fov is irrelevant, because the detection algorithm has the same sensitivity in the full field of view. So it was assumed, that video observations have the same linear dependency between *log p* and Δm but without the cutoff when *log p* approaches zero.

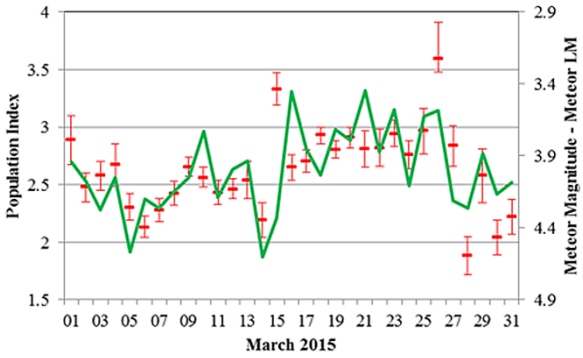

Figure 9 – Comparison of the mean difference between meteor brightness and limiting magnitude with the population index.

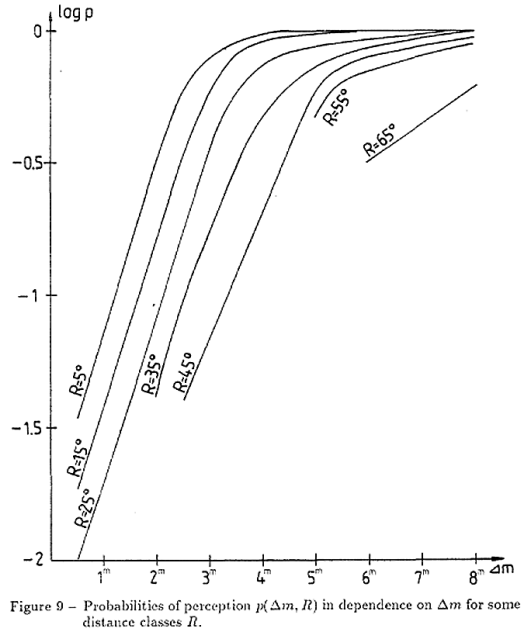

Figure 9 – Probabilities of perception $p(\Delta m, R)$ in dependence on Δm for some distance classes R.

Figure 10 – Dependency of the log detection probability *log p* for visual meteors from their brightness difference to the limiting magnitude Δm and the distance from the center of field of view R (from Koschak and Rendtel, 1990).

The transformation for visual observation has the functional form $r = a * \Delta m^b$. Since b is close to -1, the formula can be simplified to (1).

$$r = a / \Delta m. \qquad (1)$$

For video meteors, the same functional form was applied. The parameters a and b were adapted until the resulting graph matched best to the given population index profile (*Figure 11*). It turned out, that also for video observations the best exponent is close to -1, so that the formula can be simplified into the form (1). The mean squared error was smallest with a = 10.5.

In order to check if the obtained transformation function is applicable for other meteor showers as well the analysis was repeated with the April data set. The match for sporadic meteors was still reasonable, but there was only a poor match with the population index profile of the Lyrids. So the transformation cannot be used for other meteor showers as was hoped for.

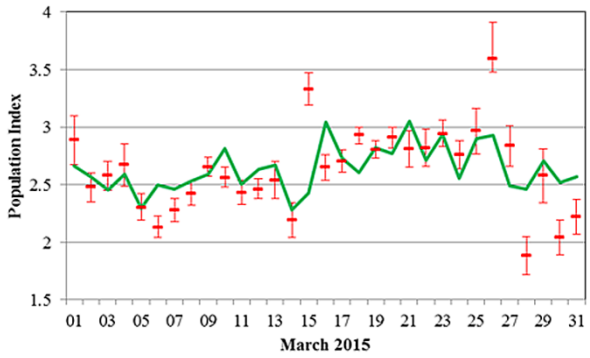

Figure 11 – Population index profile obtained from the mean difference between meteor brightness and limiting magnitude *Δm*, applying the transformation function $r=10.5/\Delta m$.

Preliminary conclusion

There are a number of potential error sources in the population index calculation proposed by Molau et al. (2014).

The limiting magnitude calculation, for example, is based on segmenting stars in the field of view which is sensitive to the segmentation threshold and other factors. Obstruction by clouds, the extinction near the horizon, lunar glare and other reasons for a variable limiting magnitude in the field of view are "transformed" into a loss of average lm which introduces further systematic errors. The limiting magnitude for meteors depends on the loss that is introduced by the angular motion of the meteor, which is non-trivial as well.

Last but not least there is by definition no "sporadic radiant", hence no sporadic radiant altitude and flux density. The empirical approach used by the MetRec software (sporadic meteors are modeled as a weighted sum of five sporadic sources) has never been revised.

These potential complex errors sources make it difficult to identify the root cause for the observed outliers in the population index profile. It might be worthwhile to look for methods where these complex error sources cancel each other out.

5 Canceling out potential error sources

You may take two video cameras with the same center of field of view, but a different limiting magnitude. Many boundary conditions like the radiant distance, angular meteor velocity, lunar distance, extinction, and cloud coverage will be the same for both cameras. The ratio of the effective collection area of the cameras (and thereby the expected meteor count ratio) depends only on the population index of the shower, as all the other factors are identical. Hence, the population index can be derived directly from the ratio of the meteor counts of both cameras. This comes as no surprise, given the definition of the population index: r is the ratio of meteor counts at different limiting magnitudes.

The test setup during the Lyrids 2015 consisted of two Mintron cameras: MINCAM1 was equipped with a 8mm f/0.8 lens, yielding a fov of 43*32° and a stellar limiting magnitude of 6 mag. ESCIMO2 was equipped with a 25mm f/0.85 lens, yielding a fov of 14*11° and a stellar limiting magnitude beyond 8 mag. Both cameras were mounted in parallel facing in southeastern direction half way to zenith.

The limiting magnitude profile of both cameras showed the expected fixed offset (*Figure 12*), and also the dependency of the collection area ratio from the population index was constant in all nights (*Figure 13*). This function simply had to be inverted (*Figure 14*) to obtain the formula (2) for the population index of the Lyrids depending from the meteor counts *n*:

$$r = 7.66 * (n_{MINCAM1} / n_{ESCIMO2})^{-0.841} \qquad (2)$$

Plugging the observed number of Lyrid meteors recorded by ESCIMO2 and MINCAM1 into the formula above did not yield a sensible population index, though. The calculation failed because the Lyrid count of ESCIMO2 remained constant between zero and two in all nights (*Figure 15*). A repetition of the experiment during the Perseids 2015 failed for technical reasons.

Poor statistics may be one possible explanation for this outcome, because the method is limited by the low meteor detection efficiency of ESCIMO2, which has a very small field of view. Another explanation may be the breakdown of the whole population index concept, which assumes that the increase of meteors by the factor r remains constant over a certain magnitude range. The observation of ESCIMO2 seems to indicate that there are simply no faint Lyrids, i.e. that r is approaching 1.0 for fainter magnitudes. For obvious reasons, this would lead to a breakdown of the proposed procedures.

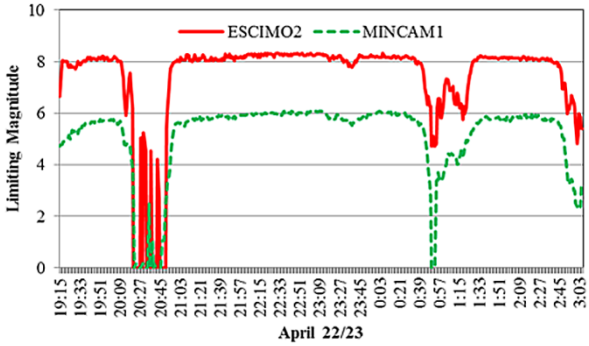

Figure 12 – Limiting magnitude profile of ESCIMO2 and MINCAM1 on April 22/23, 2015.

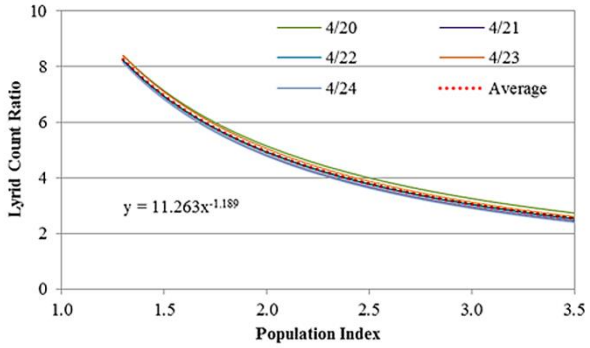

Figure 13 – Dependency of the collection area resp. expected Lyrid count ratio from the population index.

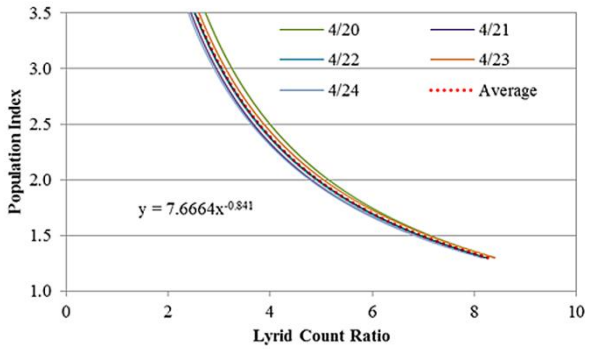

Figure 14 – Dependency of the population index from the Lyrid count ratio.

Outlook

The applied two-camera test setup still introduces uncertainties, since only the center of field of view is identical, but not the size. So effects like the radiant and lunar distance do not cancel each other out exactly. Furthermore, the relative velocity of meteors (in pixels per video frame) is different due to the different image scale. Instead of using two lenses with the *same* f-stop but *different* focal lengths one should better use two lenses with *different* f-stops but the *same* focal length. With exactly the same field of view for two cameras CAM1 and CAM2, the formula to calculate the population index would simplify to:

$$r = (n_{CAM1} / n_{CAM2})^{1/(lm_{CAM2} - lm_{CAM1})} \quad (3)$$

But it seems like a waste of equipment to point two cameras with the same field of view at exactly the same point in the sky. More favorable would be techniques that can be applied to single cameras. We need an algorithm that decides for each meteor whether or not it would have also been detected with a lower f-stop. Then we could simply simulate the second camera. This procedure would require no camera pairs and it could be applied to every single camera.

After the presentation of the talk at the 2015 IMC, a number of further ideas were discussed:

- To use liquid crystal display (LCD) shutters as presented by Bettonvil (2010) at the lens and reduce the transmission for every even or odd video field.
- To compute a synthetic video image by splitting the frame into the components meteor and noise, reducing the contribution of the meteor, and merging both components together.
- To put a threshold at the signal-to-noise-ratio (SNR) of the meteor detection and omit meteors which were below the threshold (i.e. barely detected).

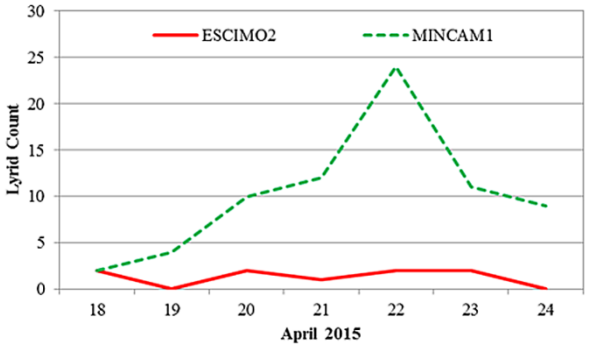

Figure 15 – Absolute number of Lyrids recorded by ESCIMO2 and MINCAM1 in April 2015.

6 Summary

Recent analyses have shown significant outliers in the population index profiles obtained by the method of Molau et al. (2014). The algorithm seems to be quite robust for the different parameters involved. It reflects the overall shape of the r profile quite well, but we should be cautious with short-term features (outliers).

It should be analyzed how the algorithm behaves when the population index is not constant in the covered lm range, as indicated from Lyrid observations in 2015.

In any case, it would be helpful to have up-to-date population index profiles from visual observations available for calibration purposes.

Acknowledgment

This work was based on video data obtained by the IMO Video Meteor Network. I would like to thank all participating observers for their valuable contribution.

References

Bettonvil F. (2010). “Digital All-sky cameras V: Liquid Crystal Optical Shutter”. In Andreić Ž. and Kac J., editors, *Proceedings of the International Meteor Conference*, Poreč, Croatia, 24-27 September 2009. IMO, pages 14–18.

Koschak R. and Rendtel J. (1990). “Determination of Spatial Number Density and Mass Index from Visual Meter Observation (I)”. *WGN, Journal of the IMO*, **18**, 44–58.

Molau S., Barentsen G. and Crivello S. (2014). “Obtaining population indices from video observations of meteors”. In Rault J. L. and Roggemans P., editors, *Proceedings of the International Meteor Conference*, Giron, France, 18–21 September 2014. IMO, pages 74–79.